Electronic Supplementary Information

Transition-metal doped titanium-oxo clusters with diverse structures and tunable photochemical properties

Dongchun Zheng†[a] , Xiao-Li Zhao†[b] , Xueqi Yan[a], Weimin Xuan[c], Qi Zheng*[a], Lianjun Wang[a,d], Wan Jiang[a,e]

[a] State Key Laboratory for Modification of Chemical Fibers and Polymer Materials & College of Materials Science and Engineering, Donghua University, Shanghai 201620, P. R. China.

[b] Shanghai Key Laboratory of Green Chemistry and Chemical Processes, Department of Chemistry, East China Normal University, 3663 North Zhongshan Road, Shanghai 200062, P. R. China.

[c] College of Chemistry, Chemical Engineering and Biotechnology, Donghua University, Shanghai 201620, China

[d] Engineering Research Center of Advanced Glasses Manufacturing Technology, Ministry of Education, Donghua University, Shanghai 201620, P. R. China

[e] Institute of Functional Materials, Donghua University, Shanghai 201620, P. R. China

Materials: $Co(CH_3COO)_2·4H_2O$ and $Mn(CH_3COO)_3·2H_2O$ were purchased from Rhawn, isopropanol, acetonitrile, methanol, ethanol and titanium tetraisopropanolate were purchased from General Reagent, Nafion and $Cd(CH_3COO)_2·2H_2O$ were purchased from Alfa and Sinopharm Chemical Reagent Co., Ltd, respectively. All reagents were of A.R. grade and used without further purification.

X-ray Crystallography: The crystallographic data of compounds were collected using a Bruker D8 venture single crystal diffractometer equipped with graphite-monochromatic Mo-Kα radiation ($\lambda = 0.71073$ Å) at 150 K. Their structures were solved and refined with OLEX2 [1], All non-hydrogen atoms are anisotropic refined by the least square method, and the hydrogen atoms are determined by the ideal geometry by the theoretical hydrogenation method. The X-ray crystallographic data for structures reported in this article have been deposited at the Cambridge Crystallographic Data Centre, under deposition number CCDC 2118622-2118624. These data can be obtained free of charge from the Cambridge Crystallographic Data Centre via www.ccdc.cam.ac.uk/data_request/cif.

Powder X-ray Diffraction (PXRD): Powder XRD was recorded on a Haoyuan DX-2700B diffractometer equipped with monochromatized Cu-Kα ($\lambda = 1.5418$ Å) radiation in the range of $3° \leq 2\theta \leq 50°$, with a scanning rate of $0.04°$ s^{-1}.

Element Analyses: Element analyses for Ti, Co, Mn and Cd were performed on a Leeman Prodigy Plus inductivity-coupled plasma Inductively Coupled Plasma Optical Emission Spectroscopy (ICP-OES) and C, N and H content were determined by VARIDEL III Elemental Analyzer.

Thermogravimetric Analysis (TGA): Thermogravimetric analysis was performed on a METTLER TOLEDO TG8000 Thermogravimetric Analyzer under nitrogen flow at a typical heating rate of 10 °C·min^{-1}.

Fourier-transform infrared (FT-IR) spectroscopy: The samples were prepared as a KBr

pellet and the FT-IR spectrum was collected in transmission mode in the range of 600-4000 cm^{-1} using a NEXUS-670 spectrometer. Wavenumbers are given in cm^{-1}. Wavenumbers are given in cm^{-1}. Intensities are denoted as w = weak, m = medium, s = strong, vs = very strong.

Solid-state UV−vis−NIR absorption spectroscopy: All compounds were prepared into powders, which were tested in wavelength mode by integrating sphere attachment in UV3600 UV-vis- NIR spectrometer.

Photocurrent Measurement: Fresh clusters (5 mg) of compounds were dispersed in 0.95 mL ethanol and 0.05 mL Nafion mixed solution. After ultrasound for about 30 min to disperse the samples, 50 μL suspensions were transferred by pipette and then dropped on the cleaned FTO glass (1×2 cm^2, 50 Ω·cm^{-2}). The photocurrent tests were carried out on a CHI650 electrochemistry workstation using a three-electrode system with a 300 W xenon lamp. The prepared FTO glass electrode was used as the working electrode, a Pt wire as the assisting electrode, and Ag/AgCl electrode as the reference electrode. A total of 100 mL of aqueous Na$_2$SO$_4$ (0.5 M) was used as the medium.

H$_2$ Evolution Experiment: The experiment was carried out in a closed gas circulation system. (Perfect Light Company Labsolar-III (AG)). A total of 50 mg of samples were dispersed in 90 mL of H$_2$O. An additional 10 mL of methanol was added as a sacrifice agent, followed by the addition 33 μL of 1.0 wt % H$_2$PtCl$_6$. A 300 W xenon lamp was used as the light source. Online gas chromatography (GC) analysis monitors the amount of H$_2$ produced at intervals of 1 h.

Synthesis of H$_2$[Ti$_2$Mn$_4$(μ$_3$-O)$_2$(Ac)$_2$(BC)$_{10}$(O^{i}Pr)$_2$]·2H$_2$O (1).

Mn(CH$_3$COO)$_3$·2H$_2$O (0.2 mmol, 53.5 mg) and benzoic acid (1 mmol, 122.1 mg) were dissolved in acetonitrile (2 mL), then acetic acid (2 μL) and Ti(O^{i}Pr)$_4$ (0.1 mL, 0.32 mmol) were added to the glass vial and mixed at room temperature. The resultant solution was heated at 80 °C for 3 days. After cooled to room temperature, Yellow rhombohedral crystal **1** were obtained. (yield: 38.01 mg, 13.60 % based on Ti(O^{i}Pr)$_4$). Anal. Calcd for C$_{80}$H$_{74}$O$_{30}$Ti$_2$Mn$_4$ (MW = 1830.91), EA: C, 52.47; H, 4.07; Ti, 5.48; Mn, 12.58, Find: C, 54.51; H, 4.70; Ti, 5.58;

Mn, 11.68. IR (KBr pellet, 4000 - 600 cm^{-1}): 3065(w), 1601(s), 1557(s), 1492(m), 1449(w), 1361(vs), 1307(w), 1176(w), 1144(w), 1104(w), 1070(w), 1025(w), 937(w), 849(w), 816(w), 715(s), 686(w), 671(m).

Synthesis of H[Ti$_8$Co$_5$(μ_2-O)(μ_3-O)$_{11}$(BC)$_{19}$(CH$_3$CN)$_2$]$_{0.5}$[Ti$_8$Co$_5$(μ_2-O)$_2$(μ_3-O)$_{10}$ (BC)$_{18}$ (H$_2$O)(CH$_3$CN)$_2$]$_{0.5}$·5CH$_3$CN (2).

Co(CH$_3$COO)$_2$·4H$_2$O (0.2 mmol, 49.8 mg) and benzoic acid (1 mmol, 122.1 mg) were dissolved in acetonitrile (2 mL), then isopropanol (200 μL), acetic acid (2 μL) and Ti(O^{i}Pr)$_4$ (0.1 mL, 0.32 mmol) were added to the glass vial and mixed at room temperature. The resultant solution was heated at 80 °C for 3-5 days. After cooled to room temperature, Purplish red rod crystals of **2** were obtained. (yield: 26.67 mg, 19.3 % based on Ti(O^{i}Pr)$_4$). Anal. Calcd for C$_{286}$H$_{224}$Co$_{10}$N$_{12}$O$_{99}$Ti$_{16}$ (MW = 6768.05), EA: C, 50.75; H, 3.36; N, 2.48; Ti, 11.07; Co, 8.52, Find: C, 49.26; H, 3.58; N, 2.42; Ti, 10.41; Co, 8.49. IR (KBr pellet, 4000-600 cm^{-1}): 3628(w), 3063(w), 2163(w), 1918(w), 1598(s), 1551(s), 1492(m), 1449(m), 1390(vs), 1331(s), 1307(m), 1177(m), 1070(w), 1025(w), 827(w), 768(w), 713(s), 687(w), 672(w).

Synthesis of [Ti$_{12}$Cd$_5$(μ_2-O)(μ_3-O)$_{15}$(μ_4-O)$_2$(BC)$_{21}$(BCA)(Ac)(CH$_3$CN)]·3CH$_3$CN (3).

Cd(CH$_3$COO)$_2$·2H$_2$O (0.2 mmol, 53.3 mg) and benzoic acid (1 mmol, 122.1 mg) were dissolved in acetonitrile (2 mL), then acetic acid (2 μL) and Ti(O^{i}Pr)$_4$ (0.1 mL, 0.32 mmol) were added to the glass vial and mixed at room temperature. The resultant solution was heated at 80 °C for 3 days. After cooled to room temperature, colorless crystals of **3** were obtained. (yield: 64.02 mg, 56.60 % based on Ti(O^{i}Pr)$_4$). Anal. Calcd for C$_{164}$H$_{126}$O$_{64}$N$_4$Ti$_{12}$Cd$_5$ (MW = 4313.20), EA: C, 45.67; H, 2.94; N, 1.30; Ti, 13.54; Cd, 13.25, Find: C, 45.18; H,3.01; N, 1.24; Ti, 13.32; Cd, 13.28. IR (KBr pellet, 4000 - 600 cm^{-1}): 3320(w), 3064(w), 2162(w), 1599(s), 1549(s), 1492(m), 1449(m), 1352(vs), 1307(v), 1176(m), 1142(w), 1105(w), 1070(w), 1025(w), 937(w), 859(w), 816(w), 715(s), 687(w), 672(w).

Table S1 Bond valence sums for the Mn ions in compound **1**

Atom	bond	bond length (Å)	Valance Mn^{II}	Valance Mn^{III}
Mn4	Mn4-O10	2.219	0.314	0.289
	Mn4-O15	2.156	0.371	0.342
	Mn4-O18	2.103	0.429	0.396
	Mn4-O19	2.188	0.341	0.315
	Mn4-O25	2.313	0.243	0.224
	Mn4-O28	2.197	0.333	0.307
SUM			2.032	1.874
Mn3	Mn3-O7	2.156	0.372	0.343
	Mn3-O7	2.217	0.316	0.291
	Mn3-O10	2.138	0.391	0.36
	Mn3-O14	2.216	0.403	0.371
	Mn3-O15	2.185	0.344	0.317
	Mn3-O17	2.146	0.382	0.352
SUM			2.207	2.035

Table S2 Crystal data and structure refinements summary for compounds **1-3**

Compound	**1**	**2**	**3**
Empirical formula	$C_{80}H_{70}Mn_4O_{28}Ti_2$	$C_{138.5}H_{107}Co_5N_{4.5}O_{49.5}Ti_8$	$C_{173}H_{119.5}Cd_{4.52}N_{8.5}O_{64}Ti_{12.48}$
Formula weight	1794.92	3304.13	4447.10
Crystal system	Monoclinic	Monoclinic	Triclinic
Space group	$P2_1/c$	Cc	$P-1$
a /Å	12.3119(4)	28.5375(10)	17.0921(6)
b /Å	15.1945(4)	18.5257(5)	20.7384(8)
c /Å	21.7763(8)	53.3966(17)	27.4498(10)
α/°	90	90	96.4130(10)
β/°	102.8930(10)	96.0990(10)	94.6680(10)
γ/°	90	90	107.9250(10)
V /Å³	3971.1(2)	28069.8(15)	9130.5(6)
Z	2	8	2
ρ calc /g·cm⁻³	1.501	1.564	1.618
μ(MoKα) /mm⁻¹	0.89	1.091	1.116
F(000)	1836	13412	4441
2θ range /°	2.681 to 25.378	1.313 to 26.390	2.079 to 25.000
Reflections collected/ unique	23524	183022	68781
Data/restraints/ parameters	7233/0/517	55477/6851/3678	31905/4608/2211
R_1/wR_2 (I>2σ(I))[a]	0.0500/0.0948	0.0446/0.1189	0.0749/0.2097
R_1/wR_2 (all data)	0.0932/0.1148	0.0484/0.1216	0.1089/0.2386
GooF (all data)[b]	1.04	1.042	1.032
Data completeness	99.30%	98.80 %	99.10 %
Max. peak/hole /e·Å⁻³	0.416/-0.418	1.176/-0.689	2.986/-1.233

[a]$R_1 = \sum||Fo|-|Fc||/\sum|Fo|$; $wR_2 = \{\sum w[(Fo)^2-(Fc)^2]^2/\sum w[(Fo)^2]^2\}^{1/2}$

[b]$GooF = \{\sum w[(Fo)^2-(Fc)^2]^2/(n-p)\}^{1/2}$
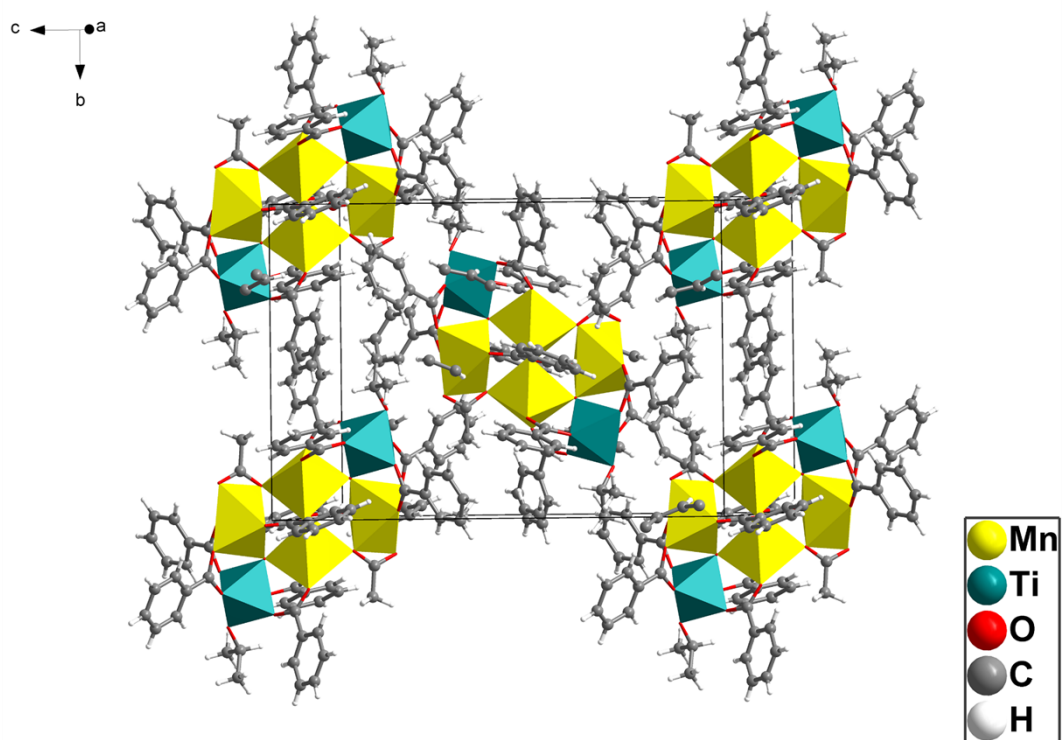
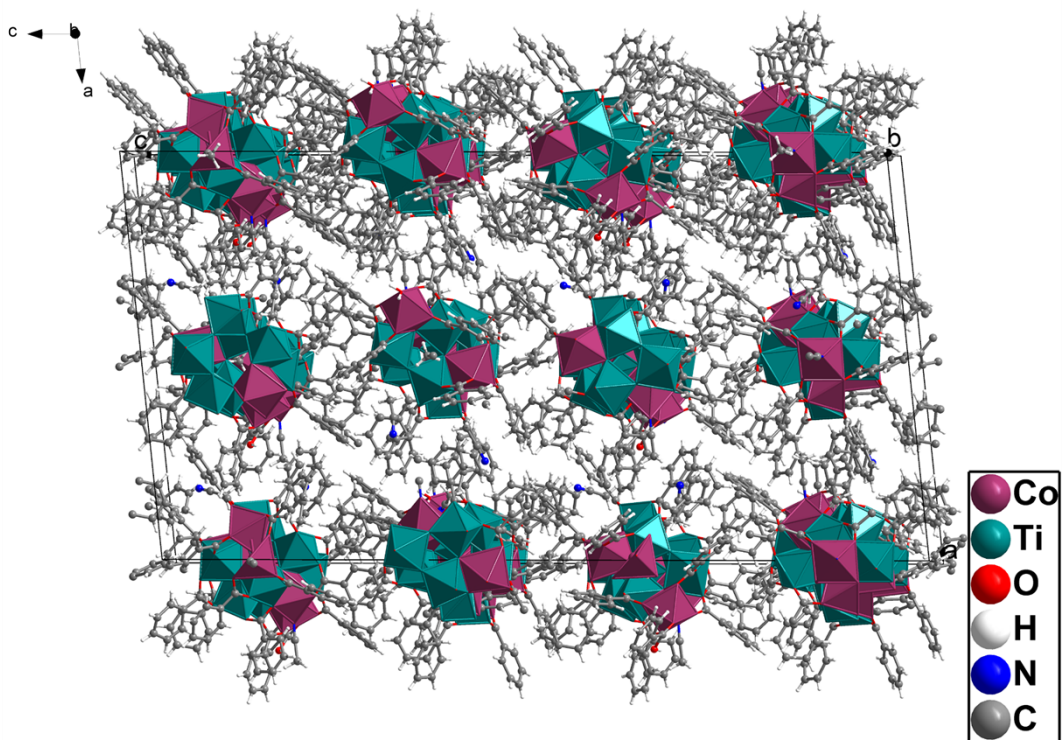Figure S1 Unit Cell packing structure of compound **1**.

Figure S2 Unit Cell packing structure of compound **2**.
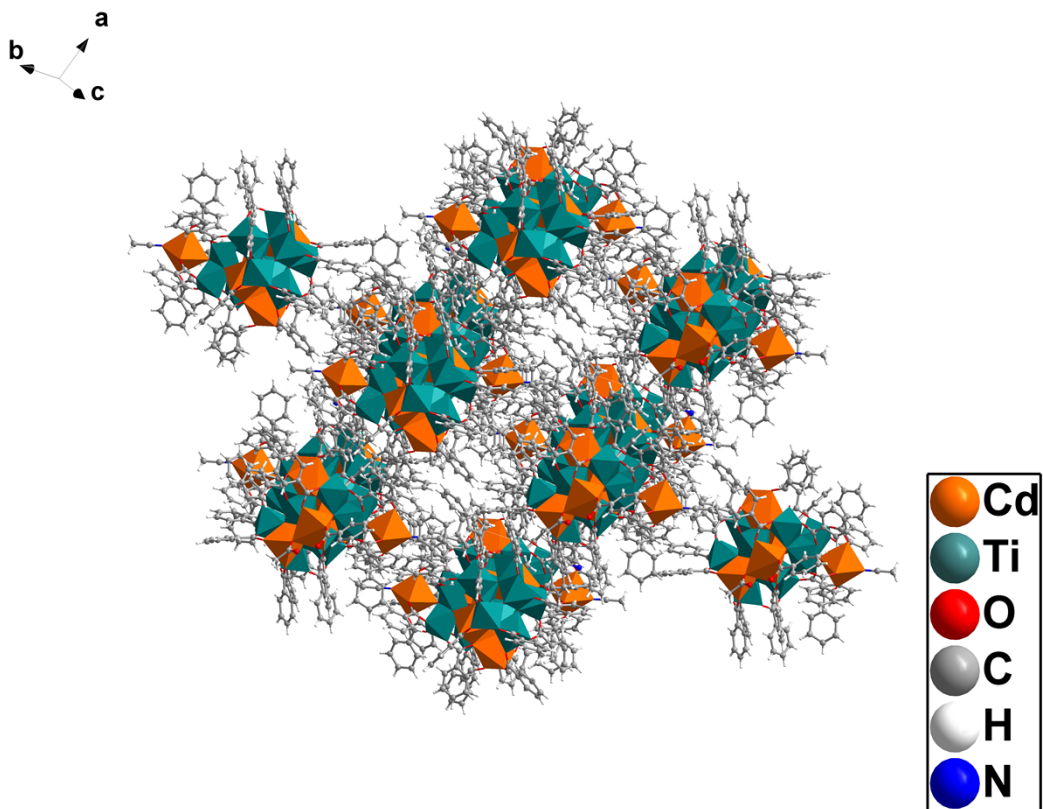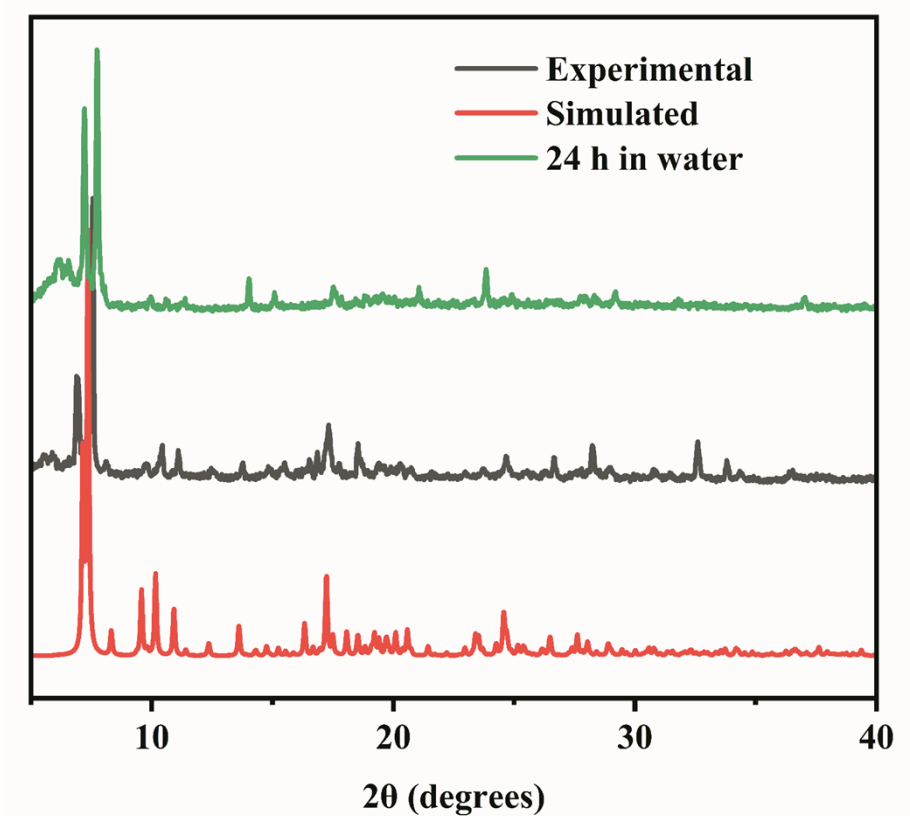
Figure S3 Packing structure of compound **3**.

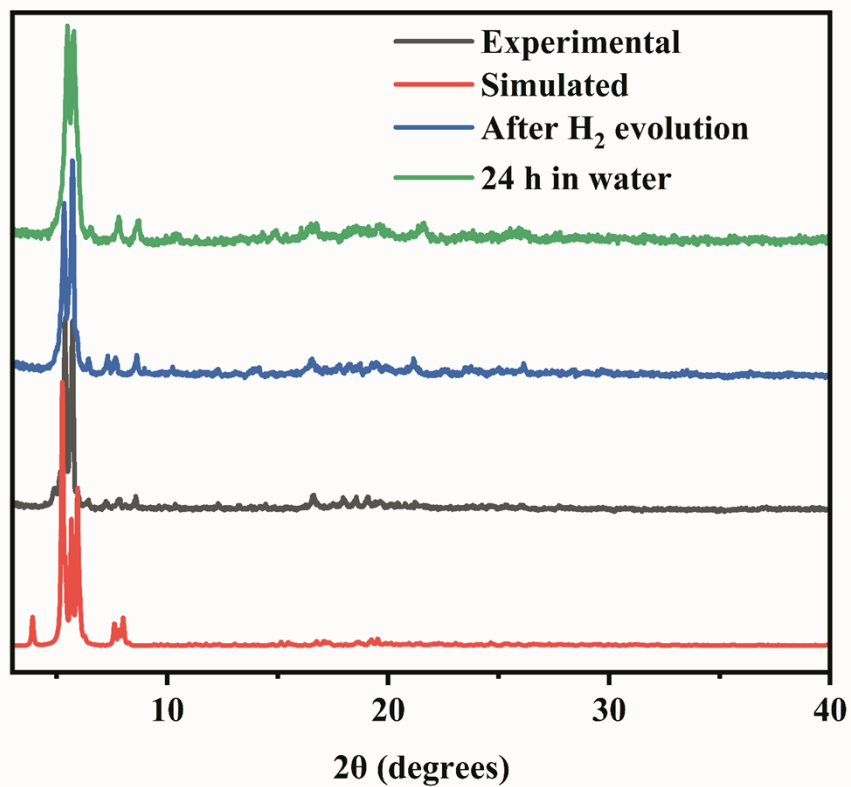Figure S4 The PXRD patterns of **1**.
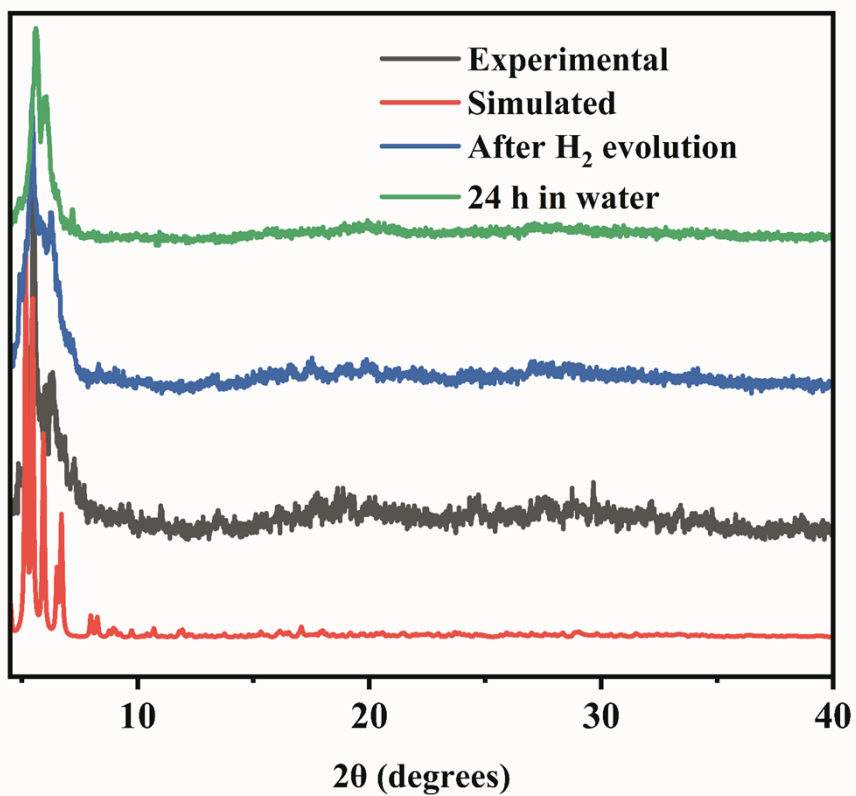
Figure S5 The PXRD patterns of **2**.
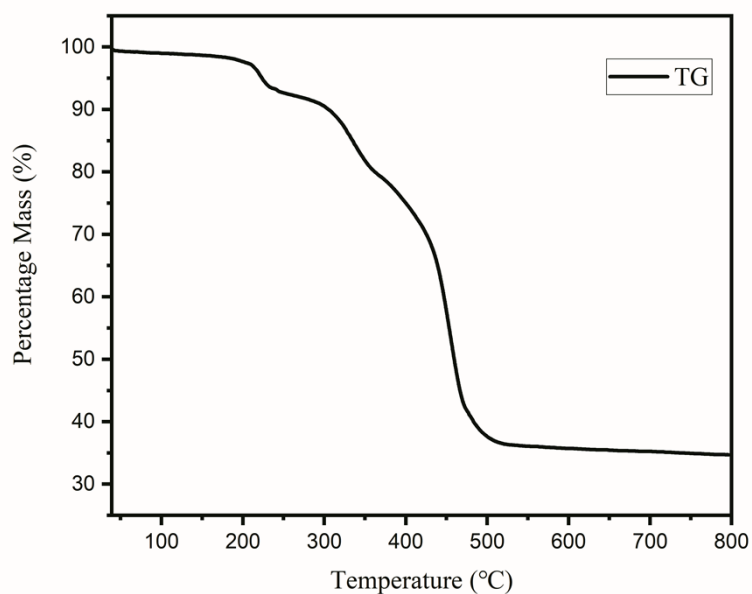

Figure S6 The PXRD patterns of **3**.

Figure S7 The thermogravimetric (TG) curve of **1**. The mass loss before 200 °C is corresponding to two guest water molecules (1.75 %), and the coordinated isopropanol molecules are lost between 240-260 °C (6.55 %). Afterwards, **1** begins to decompose and completely transforms to related metal oxide after 500 °C.
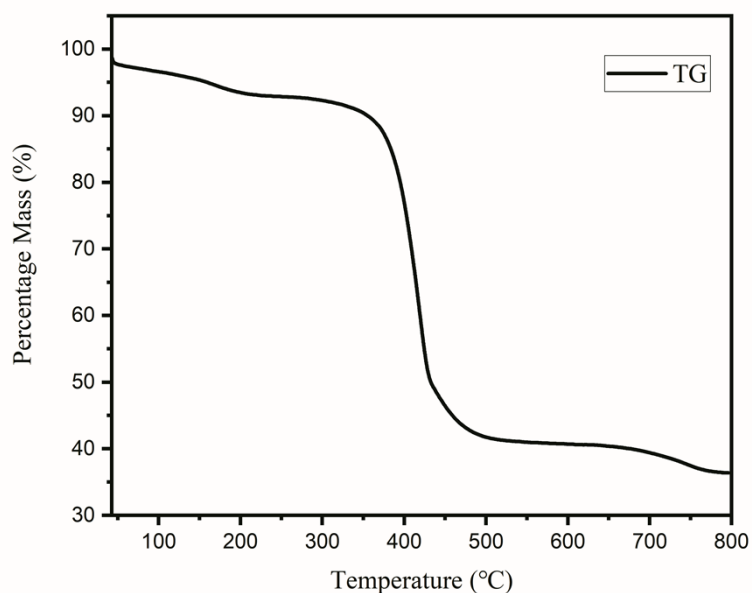
Figure S8 The thermogravimetric (TG) curve of **2**. The mass loss before 200 °C is corresponding to solvent/coordinated acetonitrile (4.2 % in total). When the temperature exceeds 380 °C, **2** begins to decompose and completely transforms to related metal oxide after 500 °C.
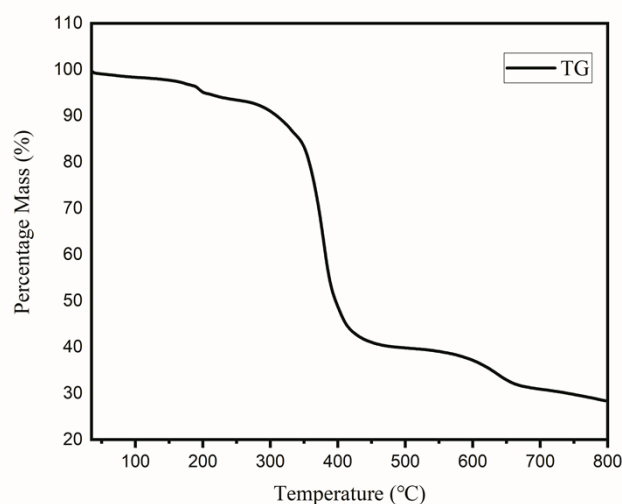
Figure S9 The thermogravimetric (TG) curve of **3**. The mass loss before 200 °C is corresponding to solvent/coordinated acetonitrile (3.8 % in total), the monodentate coordinated acetic acid is lost between 200-320 °C (4.2%). Afterwards, **1** begins to decompose and completely transforms to related metal oxide after 400 °C.
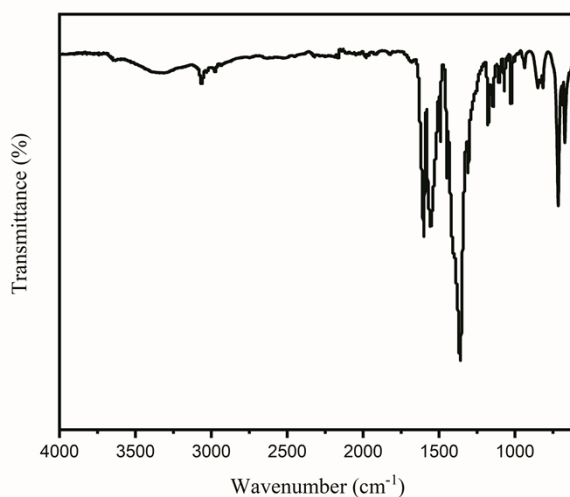

Figure S10 The FT-IR spectrum of **1**. The absorption bands between 3000−2800 cm^{-1} can be ascribed to the stretching vibrations of C-H bonds from benzene rings and alkyl groups. The characteristic stretching vibrations of carboxylate (1633−1550 cm^{-1}) and ν(C=C) in benzene rings are overlapped from 1633 cm^{-1} to 1350 cm^{-1}. Besides, the intense absorption peaks between 1100−1000 cm^{-1} are assigned to the stretching vibrations of ν(C–O) from isopropanol.
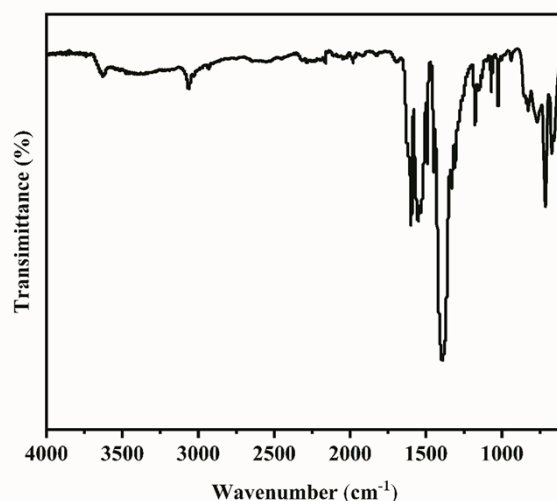
Figure S11 The FT-IR spectrum of **2**. The weak absorption bands between 3100−3000 cm^{-1} and strong absorption bands centered at 1633 cm^{-1} and 1370 cm^{-1}, which can be ascribed to the stretching vibration modes of C-H bonds in benzene rings and v(C=O) of carboxylate, v(C=C) in benzene rings, respectively. The weak absorption bands between 2250−2150 cm^{-1} can be ascribed to the stretching vibration of C≡N bonds in acetonitrile molecules.
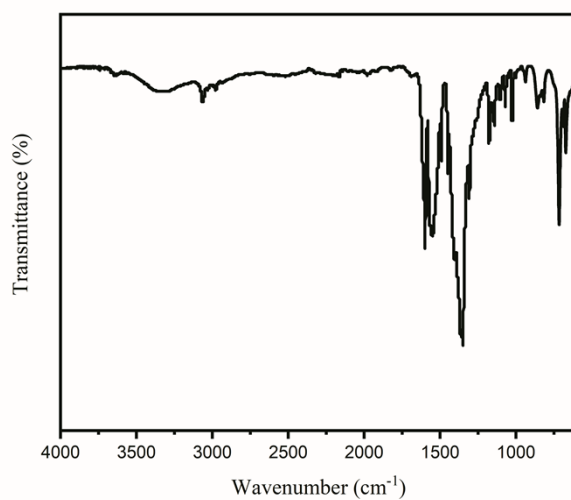

Figure S12 The FT-IR spectrum of **3**. The FT-IR spectrum of **3** is quite similar to **2**, with the absorption bands assigned in the same way. See Figure S11 for details.
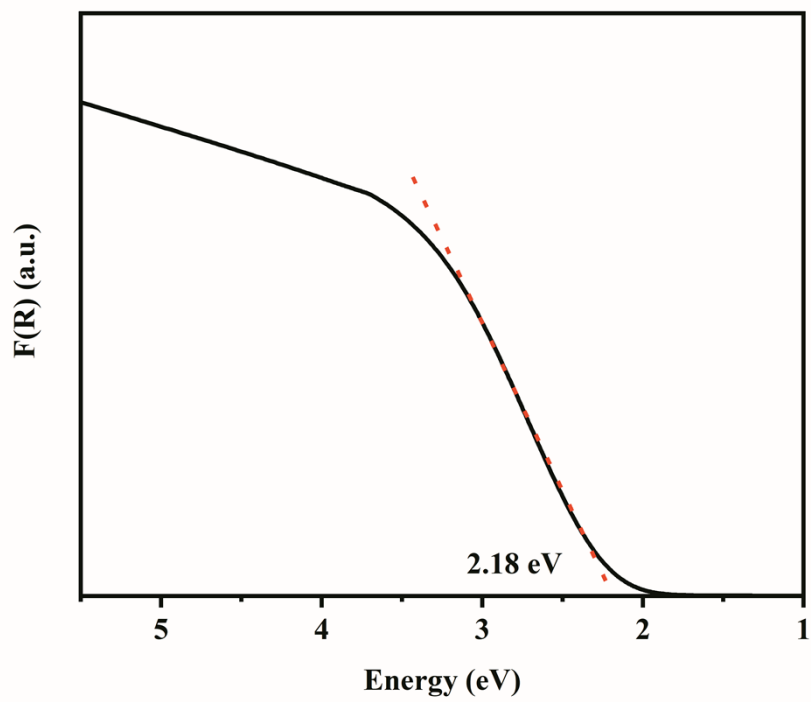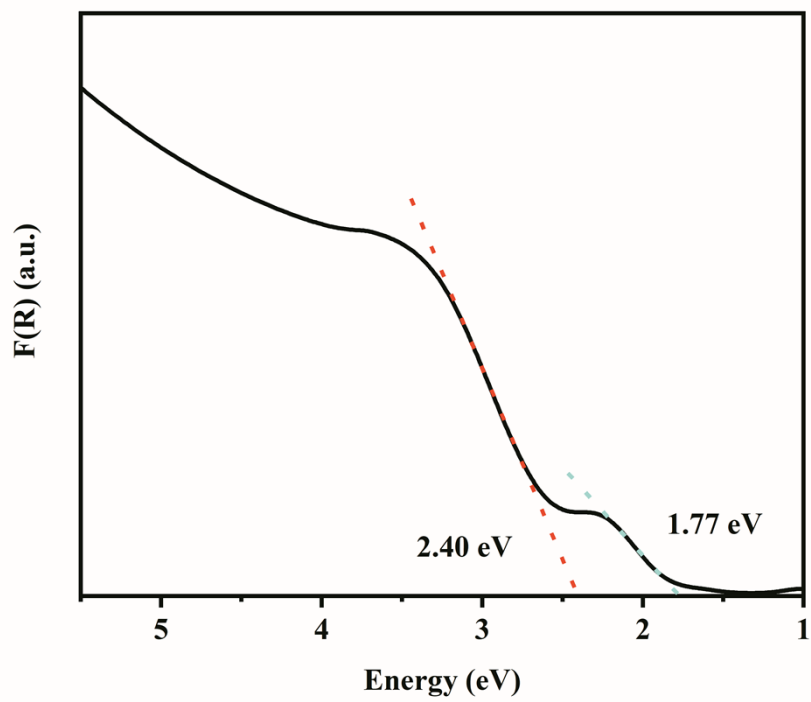
Figure S13 The band gap of **1**.

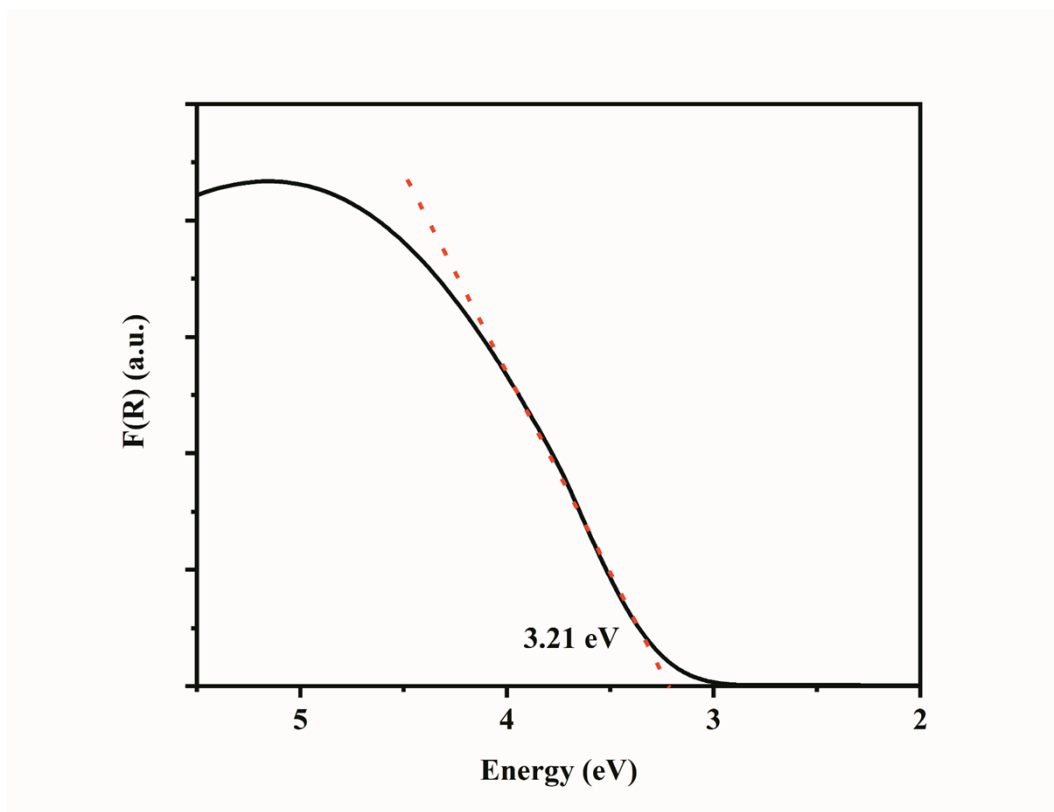Figure S14 The band gap of **2**.

Figure S15 The band gap of **3**.

Reference

[1] O. V. Dolomanov, L. J. Bourhis, R. J. Gildea, J. A. K. Howard and H. Puschmann. "OLEX2: a complete structure solution, refinement and analysis program". J. Appl. Cryst. 2009, **42**, 339-341.